Accurate calculations of 3p and 3d lifetimes in the Na sequence

Constantine E. Theodosiou and Lorenzo J. Curtis

Department of Physics and Astronomy, The University of Toledo, Toledo, Ohio 43606

(Received 2 May 1988)

Computed lifetimes for the $3p\,^2P_{1/2}$, $3p\,^2P_{3/2}$, $3d\,^2D_{3/2}$, and $3d\,^2D_{5/2}$ levels in the sodium isoelectronic sequence are presented for $Z = 11-54$, 74, 79, 90, and 92. These calculations agree well with recent high-precision lifetime measurements, and conflict with some *ab initio* estimates which indicated lifetimes shorter than those experimentally observed. Our calculations involve the inclusion of experimental energy-level data and the use of a realistic model potential, which utilizes comprehensive spectroscopic measurements that have recently become available. We also demonstrate that the core-polarization effects are significant and must be included to obtain agreement with experiment. As part of the study, we used the existing data base and Dirac-Fock methods to determine new values for ionization potentials in this sequence.

I. INTRODUCTION

Lifetimes of the *ns-np* resonance transitions in alkali-metal-like isoelectronic sequences provide a challenging confrontation between theory and experiment. Although these systems consist basically of a single electron outside closed shells, the intrashell nature of these transitions produces both theoretical and experimental subtleties. The relative positions of the levels have a strong isoelectronic variation, and the ratio of the $^2P_{1/2}$-$^2P_{3/2}$ (regular doublet) and $^2S_{1/2}$-$^2P_{1/2}$ (irregular doublet) intervals is small for low-ionization and large for high-ionization stages. This causes lifetimes and state populations of the individual fine-structure levels to have a similarly strong isoelectronic variation. Theoretically, core polarization and other types of electron correlation, spin-orbit coupling and other relativistic interactions, and the relative virtues of Breit-Pauli and fully relativistic treatments can vary with the degree of ionicity. Experimentally, these intrashell decay channels are repopulated by faster extrashell cascades and by the yrast chain, so experimental decay curves exhibit both growing-in and -out cascades. Lifetime determination by simple multiexponential fitting procedures are known to be unreliable for these systems,[1,2] and more sophisticated experimental procedures must be used.[3,4]

Elaborate theoretical calculations have been published, and high-precision measurements using methods that eliminate or exactly account for cascading have recently been reported for the 3s-3p and 3p-3d transitions in the Na isoelectronic sequence,[5-11] and discrepancies have emerged. It is the purpose of this paper to report new calculations that reproduce the observed lifetimes to within experimental accuracies, and provide precise predictions for higher members of the sequence. These computations utilize the Hartree-Slater method with a realistic potential. In order to extend the application of this method, we have also used spectroscopic data and multiconfiguration Dirac-Fock calculations to deduce additional values for ionization potentials in the Na sequence.

II. SURVEY OF PRECISE EXPERIMENTAL LIFETIME DATA

An uncritical compilation of lifetime data for 3p lifetimes in the Na sequence can be misleading, since early measurements based solely on exponential curve fitting systematically overestimated the lifetimes. Analyses that fit a sum of exponential functions to the decay curve of a heavily cascaded alkali-metal-like resonance transition almost invariably yield an overestimate of the lifetime,[1,2] and such data should be categorically excluded from comparisons with theory. The tendency of the *ns-np* experimental lifetimes to exceed theoretical estimates was for a time assumed to be totally an artifact of cascade repopulation, but it appears that some discrepancies toward longer lifetimes still exist after cascade effects have been eliminated.

Precision measurements have now been made that either exclude or properly account for cascade repopulation. One approach is to use selective excitation of a fast ion beam as a laser. Gaupp *et al.*[12] have performed high-precision (<0.2%) beam-laser measurements for the $J = \frac{1}{2}$-$\frac{1}{2}$ resonance transitions in Li I and Na I which yielded lifetimes that are several experimental standard deviations longer than those predicted by *ab initio* theory. Quantum beats from unresolved hyperfine structure precluded a precision lifetime measurement of the $J = \frac{1}{2}$-$\frac{3}{2}$ resonance transitions by this method. However, an independent measurement by Gawlik *et al.*[13] of the ratio of the 3s-3p oscillator strengths for Na permits the precise specification of the lifetimes of both fine-structure transitions. These results caused a troubling discrepancy, and concern has been expressed[7] as to whether calculational uncertainties can accommodate the differences.

The only source of direct lifetime measurements for highly ionized atomic systems is by foil excitation of a fast ion beam, which is non-state-selective. While beam-foil techniques do not yet permit measurements to within parts per thousand for highly ionized systems, methods are available that provide internal tests which insure that quoted uncertainties (nominally 5%) are realistic. Recent

measurements have utilized the arbitrarily normalized decay curve method[3,4] (ANDC) which exploits dynamical correlations among cascade-related decay curves to reliably extract lifetimes. This method utilizes the rate equation connecting the population of the nth level to that of the ith levels that cascade directly into it. Since the instantaneous time dependence of each level population is, to within constant factors involving the transition probabilities and detection efficiencies, proportional to the measured decay curve $I_{jk}(t)$, the instantaneous population equation can be written

$$\tau_n \frac{dI_{nf}}{dt} = \sum_i E_{in} I_{in}(t) - I_{nf}(t) \ . \tag{1}$$

This provides the exposition of a set of relationships between a given time point on the primary decay curve and the corresponding points on its direct cascades, with constant coefficients given by the lifetime τ_n and the relative normalization parameters E_{in}. Analysis consists of using this equation to relate measured $I_{jk}(t)$'s (using numerical differentiation or integration) to determine τ_n and the E_{in}'s through a linear regression. If all significant direct cascades have been included, the goodness of fit will be uniform for all time subregions, but if important cascades have been omitted or blends are present, the fit will vary over time subregions. For alkali-metal-like resonance transitions, cascading occurs dominantly along the yrast chain, and can often be accounted for using only a single repopulation channel. Very rugged algorithms have been developed[14,15] that permit reliable lifetimes to be extracted, even in cases where the cascade contributions are dominant, and studies of the propagation and correlation of errors have been made.[16]

A series of beam-foil lifetime measurements for ions in the Na sequence employing the ANDC method has recently been reported,[17-21] which comprises a data base against which theoretical calculations should be compared. The measurements have been performed separately on each fine-structure component to typically 5% accuracies, and include the ions S VI,[17] Cl VII,[18] Ar VIII,[19] Ti XII,[20] Fe XVI,[20,21] Ni XVIII,[20] and Cu XIX.[20] These experimental lifetimes and their quoted uncertainties are given in Table I. Earlier measurements which utilized

only curve fitting methods or determined only multiplet values (cf. bibliographic citations in Refs. 1, 12, and 17–19) may contain systematic errors which exceed quoted uncertainties, and should not be included in modern comparisons with theory.

III. SPECTROSCOPIC DATA BASE

The Hartree-Slater theoretical approach[29,30] that we have used involves the integration of the Schrödinger equation with a relativistic model potential, constrained to yield the experimental binding-energy levels. Thus it is necessary to input values both for the excitation energies of the levels in question and for the ionization limit. Reliable data for excitation energies are now available for the Na sequence through 44 stages of ionization, and these data have permitted ionization potential determinations to be extended to this degree of ionization.

Spectroscopic analysis is essentially complete for the ions Na I–Cl VII.[31-36] Precision measurements are available for most of the 3s-3p, 3p-3d, and 3d-4f transition wavelengths for the ions Ar VIII–Sn XL (as reported and summarized in Ref. 37). Reader et al.[37] have parametrized the differences between the observations and corresponding Dirac-Fock calculations, and obtained a set of fitted values for Ar VIII–Xe XLIV. By combining these large blocks of slowly varying isoelectronic data, they have obtained a semiempirical systematization of the data that is expected to be more accurate than the individual measurements that make it up, yielding a quoted uncertainty of less than ±0.07 Å.

In 1979 Edlén[38] made a systematic study of the ionization potentials, and we have now updated this work using the new measurements in Ref. 37. The ionization potentials can be obtained from the 3s-3p-3d-4f transition wavelengths by establishing the excitation energies of the 4f levels, and adding to them the 4f term energies as predicted by the core polarization model (using extrapolated effective dipole and quadrupole polarizabilities given by Edlén[38]). Since they were based on two or more nf levels, we have retained the ionization potentials deduced by Edlén for $Z < 30$, but we have replaced or augmented his results with new determinations for $30 \le Z \le 54$ (given in Table II) using the data in Ref. 37, with center-of-gravity

TABLE I. Comparison of the available ANDC-type and cascade-free $3p\ ^2P$ and $3d\ ^2D$ lifetime measurements with the present and Dirac-Fock calculations for the Na isoelectronic sequence.

		Experiment		Theory	
Ion	Level	ANDC	Other	Present	DF[a]
Na I	$3p\ ^2P_{1/2}$		16.40(3)[b]	16.399	17.92
	$3p\ ^2P_{3/2}$		16.12(22)[b,c]	16.352	17.86
Mg II	$3p\ ^2P_{1/2}$			3.872	3.937
	$3p\ ^2P_{3/2}$		4.0(3)[d]	3.842	3.906
	$3d\ ^2D_{3/2}$			2.067	
	$3d\ ^2D_{5/2}$		2.2(2)[d]	2.076	

TABLE I. (Continued).

Ion	Level	Experiment		Theory	
		ANDC	Other	Present	DF[a]
S VI	$3p\,^2P_{1/2}$	$0.59(2)^e$		0.618	
	$3p\,^2P_{3/2}$	$0.60(2)^e$		0.596	
	$3d\,^2D_{3/2}$	$0.20(1)^e$		0.197	
	$3d\,^2D_{5/2}$	$0.22(2)^e$		0.201	
Cl VII	$3p\,^2P_{1/2}$	$0.51(2)^f$		0.493	
	$3p\,^2P_{3/2}$	$0.47(1)^f$		0.470	
	$3d\,^2D_{3/2}$		$0.19(2)^f$	0.158	
	$3d\,^2D_{5/2}$		$0.17(1)^f$	0.163	
Ar VIII	$3p\,^2P_{1/2}$	$0.417(10)^g$	$\begin{cases}0.40(10)^h\\0.423(40)^i\end{cases}$	0.409	0.389
	$3p\,^2P_{3/2}$	$\begin{cases}0.389(10)^g\\0.428(27)^h\end{cases}$	$\begin{cases}0.427(30)^h\\0.421(40)^i\end{cases}$	0.386	0.366
	$3d\,^2D_{3/2}$		$\begin{cases}0.158(8)^h\\0.130(5)^i\end{cases}$	0.134	
	$3d\,^2D_{5/2}$		$\begin{cases}0.160(8)^h\\0.131(5)^i\end{cases}$	0.138	
Ti XII	$3p\,^2P_{1/2}$	$0.241(15)^j$		0.236	
	$3p\,^2P_{3/2}$	$0.204(13)^j$		0.208	
	$3d\,^2D_{3/2}$		0.110^j	0.082	
	$3d\,^2D_{5/2}$		0.102^j	0.087	
Fe XVI	$3p\,^2P_{1/2}$	$\begin{cases}0.170(11)^j\\0.167(11)^l\end{cases}$	$0.157(10)^k$	0.162	0.154
	$3p\,^2P_{3/2}$	$\begin{cases}0.138(9)^j\\0.135(8)^l\end{cases}$		0.129	0.123
	$3p\,^2P_{3/2}$	0.138^k			
	$3d\,^2D_{3/2}$		$\begin{cases}0.051(11)^l\\0.064(10)^j\\0.067(4)^k\end{cases}$	0.057	
	$3d\,^2D_{5/2}$		$\begin{cases}0.069(10)^l\\0.072(5)^j\\0.083(5)^k\end{cases}$	0.064	
Ni XVIII	$3p\,^2P_{1/2}$	$0.141(9)^j$	$0.137(14)^m$	0.139	
	$3p\,^2P_{3/2}$	$0.113(8)^j$	$0.108(11)^m$	0.104	
	$3d\,^2D_{3/2}$		$\begin{cases}0.054(2)^j\\0.066(7)^m\end{cases}$	0.049	
	$3d\,^2D_{5/2}$		$0.062(2)^j$	0.056	
Cu XIX	$3p\,^2P_{1/2}$	$0.123(8)^j$	$\begin{cases}0.085(18)^n\\0.123(4)^o\end{cases}$	0.130	
	$3d\,^2D_{3/2}$		$\begin{cases}0.031(3)^j\\0.054(6)^n\\0.041(2)^o\end{cases}$	0.045	

[a]Y.-K. Kim and K.-T. Cheng, Ref. 6.
[b]A. Gaupp et al., Ref. 12; Refs. 12 and 22 provide a comprehensive bibliography for the Na states.
[c]W. Gawlik et al., Ref. 12.
[d]L. Lundin et al., Ref. 22.
[e]J. O. Ekberg et al., Ref. 17.
[f]C. Jupén et al., Ref. 18.
[g]N. Reistad et al., Ref. 19.
[h]E. H. Pinnington et al., Ref. 23.
[i]M. C. Buchet-Poulizac et al., Ref. 24.
[j]R. Hutton et al., Ref. 20.
[k]J. P. Buchet et al., Ref. 21.
[l]R. Hutton et al., Ref. 25.
[m]D. J. Pegg et al., Ref. 26.
[n]D. J. Pegg et al., Ref. 27.
[o]M. C. Buchet-Poulizac and J. P. Buchet, Ref. 28.

TABLE II. Ionization potentials (IP), in cm^{-1}, deduced herein for $Z \geq 30$. Values for $Z < 30$ were taken from Refs. 31–36 and 38.

Z	IP	Z	IP
30	5 947 326[a]	45	17 166 876[b]
31	6 511 265[a]	46	18 139 451[b]
32	7 101 287[a]	47	19 132 927[b]
33	7 717 227[a]	48	20 154 028[b]
34	8 359 481[a]	49	21 203 787[b]
35	9 027 754[a]	50	22 285 181[a]
36	9 721 010[a]	51	23 390 044[b]
37	10 441 573[b]	52	24 526 763[b]
38	11 188 540[a]	53	25 692 796[b]
39	11 961 100[a]	54	26 888 768[b]
40	12 761 077[a]	74	57 523 696[c]
41	13 589 777[a]	79	67 523 825[c]
42	14 445 999[a]	90	92 880 985[c]
43	15 327 450[b]	92	98 220 914[c]
44	16 237 208[a]		

[a]Deduced from measured $3s$-$3p$-$3d$-$4f$ intervals in Ref. 37 and polarization parameters from Ref. 38.

[b]Deduced from fitted $3s$-$3p$-$3d$-$4f$ intervals in Ref. 37 and polarization parameters from Ref. 38.

[c]Deduced from extrapolated differences between the values given above and present theoretical MCDF calculations.

weighting for the $4f$ fine-structure levels. Brown et al.[39] have applied the same type of analysis to their data for Se XXIV, which includes $5f$ and $5g$ in addition to $4f$. Their adopted ionization potential (8 358 700 ± 1000)cm^{-1} compares well to our value 8 359 481 cm^{-1}, and indicates that the $4f$ data are adequate for this specification.

We have also extrapolated both the excitation energies and the ionization potentials for a few very high Z values. Ab initio multiconfiguration Dirac-Fock (MCDF) calculations[40] were made for these quantities, and the difference between MCDF and observed values for $Z \geq 54$ were extrapolated to $Z = 74, 79, 90$, and 92.

IV. THEORETICAL FORMULATION

A large number of types of calculations has been made for this sequence, but each suffers from limitations. Ab initio Dirac-Fock (DF) calculations[6] treat the fine structure of $3p$ levels in a fully relativistic manner, which is very important for high stages of ionization. However, these calculations do not adequately describe correlation effects, and show large disagreements with experiment. Nonrelativistic multiconfiguration Hartree-Fock calculations have been made[5] which include electron-correlation corrections. However, the lifetime results obtained in this manner are not truly ab initio, since only a single value for the line strength is obtained for both $3p$ levels, and the experimental wavelengths must be used to obtain level lifetimes. Semiempirical calculations have also been

performed, using, e.g., the Coulomb approximation.[41] While these calculations sometimes yield striking agreement with experiment, they are not ab initio, and require spectroscopic data as input.

One difficulty in selecting between a fully relativistic treatment without electron correlation and a nonrelativistic treatment with correlation is shown in Fig. 1. Here the theoretical values for the ratio of the line strengths $S(\frac{1}{2}, \frac{3}{2})/S(\frac{1}{2}, \frac{1}{2})$ for the fine-structure transitions are plotted versus nuclear charge. In the nonrelativistic limit, this ratio would be exactly 2, and the ratio of the two lifetimes would be proportional to the cube of the wavelength ratio. For low Z this is nearly true, and the deviation from 2 is less than 1% for elements up to and including the iron group. For higher Z the deviation becomes larger, and (neglecting effects of correlation) exceeds 15% for $Z > 80$. It is interesting to note that for neutral sodium this ratio has been shown experimentally[13] to be 1.983 ± 0.004. The DF calculations of Ref. 6 and our present calculations yield a value 1.999 for Na I, but predict that this ratio is greater than 2 for all but the neutral member of this sequence.

V. THE PRESENT APPROACH

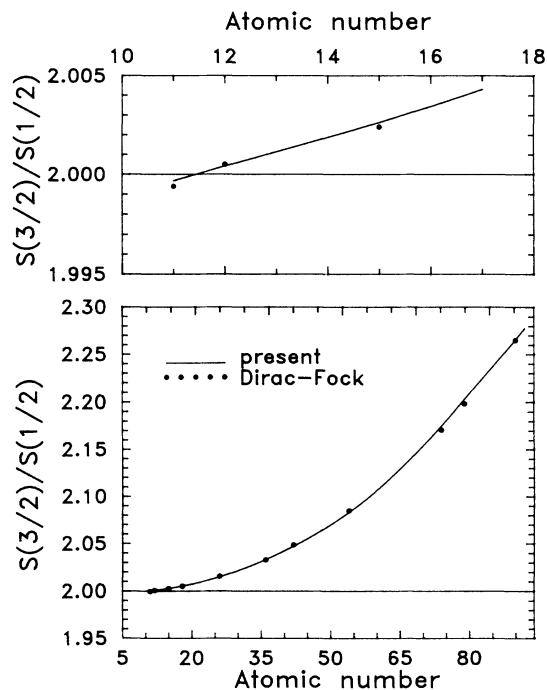The approach employed in this work was detailed in Ref. 29. Here we repeat the general features. The atomic

FIG. 1. Plot of the ratio of theoretical line strengths vs nuclear charge for the two $3s$-$3p$ fine-structure transitions in the Na isoelectronic sequence. The solid line denotes the Hartree-Slater calculations reported here and the solid circles the DF calculations of Kim and Cheng (Ref. 6).

potential used in Schrödinger's equation within the present treatment is

$$V(r) = V_c(r) + V_p(r) + V_{so}(r) , \qquad (2)$$

and consists of the following three terms.

(i) The single-electron central field V_c due to the nucleus and the core electrons, which is calculated within the Hartree-Slater approximation.[30]

(ii) The polarization potential V_p which represents the effect of the induced core electron moments on the active electron, and is taken to be of the form

$$V_p(r) = -\tfrac{1}{2}\alpha_d r^{-4}\{1 - \exp[-(r/r_1)^6]\}$$

$$+ (c_0 + c_1 r)\exp(-r/r_0) , \qquad (3)$$

where the static polarizabilities α_d were calculated by Johnson et al.,[42] r_0 is taken to be equal to the expectation value $\langle r \rangle$ of the 2p electron, and r_1 is taken to be equal to the core radius as predicted by the Hartree-Slater approximation.[30] c_0 and c_1 are adjustable parameters obtained by iteration so that the "model" potential [Eq. (2)] reproduces the experimental binding energies of the lowest 5–10 energy levels (if available) of the active electron. The fitting procedure always attained better than 1% accuracy for these energies.

(iii) The spin-orbit interaction potential V_{so} is taken to be the term in the Pauli equation. The full relativistic form is used to ensure that the potential has the correct behavior near the origin, and is given by

$$V_{so}(r) = \tfrac{1}{2}\alpha^2 f(r)^2 (1/r)[dV_m(r)/dr]\mathbf{L \cdot S} , \qquad (4)$$

with

$$f(r) = \{1 + (\alpha^2/4)[E - V_m(r)]\}^{-1} . \qquad (5)$$

Here $V_m = V_c + V_p$ is the (model) potential consisting of the core plus the polarization potentials, and has the following limiting values:

$$V_m(r=0) = -2Z/r ,$$
$$V_m(r \to \infty) = -2(Z - N)/r . \qquad (6)$$

After establishing the potential $V_{nlj}(r) = V_c + V_p + V_{so}$ we employ the experimental energy level values and integrate Schrödinger's equation

$$\frac{d^2 P_{nlj}}{dr^2} = \left[V_{nlj}(r) + \frac{l(l+1)}{r^2} - E_{nlj} \right] P_{nlj}(r) \qquad (7)$$

inwards with the correct boundary condition at

infinity.[29,43] Since we use an accurate potential the wave functions so obtained are accurate also at and near the origin. This is ensured by matching the inward integration with the outward one at the *inner* classical turning point, i.e., near the origin. The energy $E = E_{nlj}$ is an input quantity and no iterative procedure is implemented in the solution of the wave equation. Since we do not iterate the process, this numerical wave function may have a discontinuous first derivative at the matching point. The latter's location, however, is very close to the origin and has no noticeable effect on the transition matrix elements. In any case, the wave function is accurately described for most of the distances, independent of what potential is used to describe the core and polarization effects. In the low-r region we still use an accurate potential, obtained by fitting experimental energies, or, in the worst case, by a Hartree-Slater potential, which for all practical purposes is a good approximation to the "exact" potential. Still, any departure from the "exactness" consistent with the experimental energy will cause the wave function to miss passing through the origin, though the latter is a physical requirement. This difficulty is avoided by the matching of the inward integration with the outward integration at the innermost classical turning point. Figure 2 shows the calculated 3s and $3p_{1/2}$ wave functions of Ti XII as a typical example. The figure gives two sets of curves, one using the model potential described above and one obtained essentially within the Coulomb approximation (CA), i.e., by using $V(r) = -2\zeta/r$ throughout, where ζ is the asymptotic charge. We notice that the
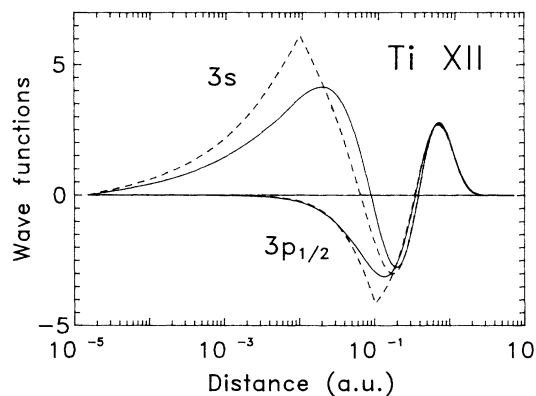

FIG. 2. Calculated 3s and $3p_{1/2}$ radial wave functions $[rR(r)]$ for Ti XII. Solid lines, using the model potential described in the text. Dashed lines, using the potential $V(r) = -24/r$ (Coulomb approximation). Notice that the discontinuities of the CA-wave-function derivatives result from the matching procedure, described in the text, at the inner classical turning point. In the traditional (analytic) Coulomb approximation both the 3s and 3p wave functions miss the origin and diverge. The model-potential wave functions are impressively smooth, although they were obtained noniteratively.

model-potential wave functions are very smooth, whereas the CA ones have a discontinuity in their derivative (due to the matching at the turning point).

Because of the inward nature of this approach, the spin-orbit interaction potential, being mainly of short range, has minimal effects on the obtained results. Nevertheless, effects of the spin-orbit interaction are inherently included into the treatment through the experimental energies employed, which depend on it directly.

The transition probability and absorption oscillator strength between two states $|\gamma J\rangle$ and $|\gamma'J'\rangle$ are given by

$$A(\gamma J \rightarrow \gamma'J') = \frac{\alpha^3}{6}\left[\frac{\Delta E}{R}\right]^3 \frac{S(\gamma J, \gamma'J')}{2J+1} \tag{8}$$

and

$$f(\gamma'J' \rightarrow \gamma J) = \frac{1}{3}\frac{\Delta E}{R}\frac{S(\gamma J, \gamma'J')}{2J'+1} , \tag{9}$$

respectively, where

$$S(\gamma J, \gamma'J') = S(nlj \rightarrow n'l'j')$$

$$= (2j+1)(2j'+1)\begin{Bmatrix} 1 & l & l' \\ \frac{1}{2} & j' & j \end{Bmatrix}^2 \max(l,l')$$

$$\times \int_0^\infty dr\, P_{nlj}(r)rP_{n'l'j'}(r) \tag{10}$$

is the line strength, α is the fine structure constant, R is the reduced-mass Rydberg energy constant, and $\Delta E = E(\gamma J) - E(\gamma'J')$ is the transition energy.

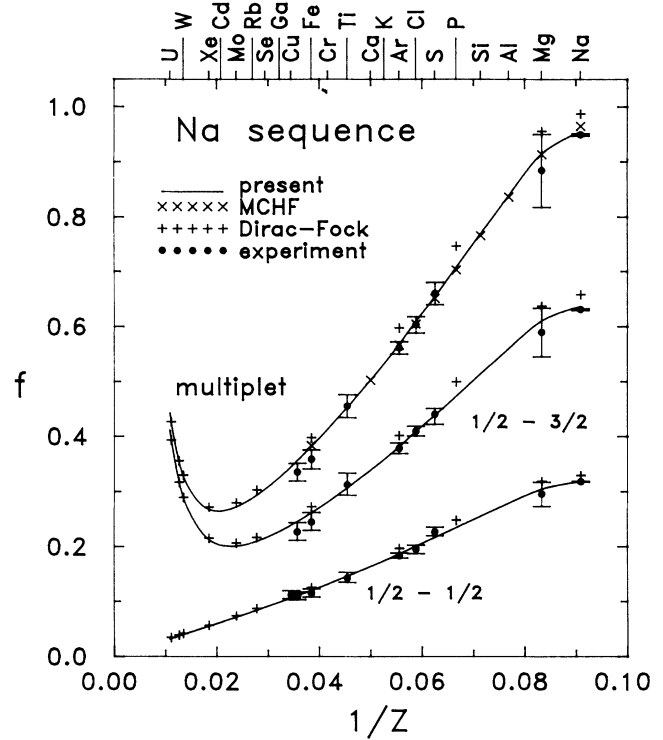The effects of core polarization by the valence electron lead to the replacement[44,45]

FIG. 3. Plot of experimental and theoretical values for the line and multiplet absorption oscillator strengths vs reciprocal of the atomic number. Solid lines trace the Hartree-Slater calculations reported here; + denotes the DF calculations of Kim and Cheng (Ref. 6), × denotes the MCHF multiplet calculations of Froese-Fischer (Ref. 5), and the experimental points are from Refs. 12-22.

TABLE III. Theoretical lifetimes for $3p_{1/2,3/2}$ and oscillator strengths for the $3s$-$3p_{1/2,3/2}$ transitions of the Na isoelectronic sequence.

| Atom | Z | Lifetime (ns) | | f | |
		$3p_{1/2}$	$3p_{3/2}$	s-$p_{1/2}$	s-$p_{3/2}$
Na	11	16.398 71	16.351 54	0.317 96	0.636 46
Mg	12	3.872 22	3.841 76	0.304 29	0.610 27
Al	13	1.865 65	1.840 45	0.278 83	0.560 41
Si	14	1.155 83	1.132 63	0.255 22	0.514 23
P	15	0.814 04	0.791 47	0.234 33	0.473 48
S	16	0.618 47	0.595 80	0.216 25	0.438 42
Cl	17	0.493 06	0.469 99	0.200 95	0.408 95
Ar	18	0.409 47	0.385 61	0.186 54	0.381 29
K	19	0.348 10	0.323 24	0.174 38	0.358 23
Ca	20	0.301 24	0.275 36	0.163 98	0.338 75
Sc	21	0.264 47	0.237 55	0.154 92	0.322 03
Ti	22	0.235 74	0.207 65	0.146 45	0.306 52
V	23	0.212 05	0.182 80	0.139 01	0.293 18
Cr	24	0.192 75	0.162 27	0.132 05	0.280 83
Mn	25	0.176 15	0.144 51	0.125 98	0.270 37
Fe	26	0.162 00	0.129 22	0.120 44	0.261 03
Co	27	0.149 78	0.115 90	0.115 38	0.252 72
Ni	28	0.139 13	0.104 20	0.110 73	0.245 34
Cu	29	0.129 96	0.093 98	0.106 29	0.238 40
Zn	30	0.121 65	0.084 74	0.102 35	0.232 56
Ga	31	0.114 24	0.076 47	0.098 69	0.227 38

ACCURATE CALCULATIONS OF 3p AND 3d LIFETIMES IN . . .

TABLE III. (Continued).

Atom	Z	Lifetime (ns)		f	
		$3p_{1/2}$	$3p_{3/2}$	s-$p_{1/2}$	s-$p_{3/2}$
Ge	32	0.107 59	0.069 04	0.095 29	0.222 79
As	33	0.101 59	0.062 35	0.092 12	0.218 74
Se	34	0.096 14	0.056 30	0.089 16	0.215 20
Br	35	0.091 18	0.050 83	0.086 39	0.212 11
Kr	36	0.086 64	0.045 86	0.083 80	0.209 46
Rb	37	0.082 47	0.041 36	0.081 35	0.207 20
Sr	38	0.078 73	0.037 32	0.078 95	0.205 05
Y	39	0.075 16	0.033 61	0.076 80	0.203 51
Zr	40	0.071 85	0.030 24	0.074 76	0.202 31
Nb	41	0.068 77	0.027 18	0.072 82	0.201 40
Mo	42	0.065 90	0.024 42	0.070 99	0.200 78
Tc	43	0.063 21	0.021 91	0.069 26	0.200 46
Ru	44	0.060 68	0.019 64	0.067 61	0.200 40
Rh	45	0.058 26	0.017 57	0.066 11	0.200 77
Pd	46	0.056 08	0.015 74	0.064 56	0.201 01
Ag	47	0.053 98	0.014 07	0.063 13	0.201 67
Cd	48	0.052 04	0.012 58	0.061 71	0.202 34
In	49	0.050 15	0.011 22	0.060 42	0.203 45
Sn	50	0.048 31	0.010 00	0.059 25	0.205 00
Sb	51	0.046 61	0.008 90	0.058 07	0.206 53
Te	52	0.044 99	0.007 93	0.056 94	0.208 26
I	53	0.043 45	0.007 05	0.055 85	0.210 19
Xe	54	0.041 98	0.006 27	0.054 82	0.212 31
W	74	0.022 60	0.000 56	0.039 62	0.286 82
Au	79	0.019 58	0.000 31	0.037 12	0.315 87
Th	90	0.014 48	0.000 08	0.032 51	0.394 76
U	92	0.013 76	0.000 07	0.031 76	0.411 51

TABLE IV. Theoretical lifetimes for $3d_{3/2,5/2}$ and oscillator strengths for the $3p_{1/2,3/2}$-$3d_{3/2}$ and $3p_{3/2}$-$3d_{5/2}$ transitions of the Na isoelectronic sequence.

Atom	Z	Lifetime (ns)		f		
		$3d_{3/2}$	$3d_{5/2}$	$p_{1/2}$-$d_{3/2}$	$p_{3/2}$-$d_{3/2}$	$p_{3/2}$-$d_{5/2}$
Na	11	19.633 66	19.664 57	0.852 93	0.085 37	0.768 36
Mg	12	2.067 20	2.075 69	0.942 66	0.094 29	0.848 62
Al	13	0.719 03	0.724 18	0.897 28	0.089 65	0.806 80
Si	14	0.390 36	0.394 56	0.808 14	0.080 62	0.725 56
P	15	0.262 24	0.266 14	0.715 78	0.071 28	0.641 56
S	16	0.197 28	0.201 18	0.634 68	0.063 06	0.567 75
Cl	17	0.158 46	0.162 47	0.567 24	0.056 22	0.506 29
Ar	18	0.133 75	0.137 99	0.507 35	0.050 14	0.451 69
K	19	0.115 60	0.120 06	0.459 70	0.045 28	0.408 16
Ca	20	0.101 66	0.106 39	0.420 75	0.041 29	0.372 42
Sc	21	0.090 47	0.095 49	0.388 74	0.037 98	0.342 90
Ti	22	0.081 66	0.087 01	0.360 14	0.035 02	0.316 46
V	23	0.074 14	0.079 81	0.336 32	0.032 53	0.294 29
Cr	24	0.067 83	0.073 85	0.315 24	0.030 31	0.274 59
Mn	25	0.062 21	0.068 57	0.297 50	0.028 42	0.257 85
Fe	26	0.057 26	0.063 97	0.282 00	0.026 75	0.243 10
Co	27	0.052 85	0.059 90	0.268 42	0.025 27	0.230 04
Ni	28	0.048 87	0.056 26	0.256 45	0.023 94	0.218 41
Cu	29	0.045 31	0.053 05	0.245 54	0.022 72	0.207 73
Zn	30	0.042 00	0.050 06	0.236 21	0.021 65	0.198 38
Ga	31	0.038 95	0.047 33	0.227 87	0.020 67	0.189 95
Ge	32	0.036 15	0.044 82	0.220 44	0.019 78	0.182 28
As	33	0.033 53	0.042 50	0.213 86	0.018 97	0.175 33
Se	34	0.031 11	0.040 34	0.207 95	0.018 21	0.168 96
Br	35	0.028 84	0.038 33	0.202 73	0.017 53	0.163 13

TABLE IV. (Continued).

Atom	Z	Lifetime (ns)		$p_{1/2}$-$d_{3/2}$	f	
		$3d_{3/2}$	$3d_{5/2}$	$p_{1/2}$-$d_{3/2}$	$p_{3/2}$-$d_{3/2}$	$p_{3/2}$-$d_{5/2}$
Kr	36	0.026 74	0.036 44	0.198 03	0.016 88	0.157 81
Rb	37	0.024 77	0.034 67	0.193 85	0.016 29	0.152 89
Sr	38	0.022 95	0.033 05	0.189 86	0.015 72	0.148 15
Y	39	0.021 22	0.031 48	0.186 64	0.015 20	0.143 96
Zr	40	0.019 60	0.029 97	0.183 78	0.014 72	0.140 15
Nb	41	0.018 08	0.028 55	0.181 29	0.014 27	0.136 59
Mo	42	0.016 66	0.027 20	0.179 15	0.013 85	0.133 31
Tc	43	0.015 32	0.025 91	0.177 38	0.013 46	0.130 25
Ru	44	0.014 08	0.024 67	0.175 85	0.013 09	0.127 48
Rh	45	0.012 91	0.023 47	0.174 78	0.012 75	0.125 00
Pd	46	0.011 85	0.022 38	0.173 57	0.012 40	0.122 42
Ag	47	0.010 84	0.021 30	0.172 90	0.012 09	0.120 16
Cd	48	0.009 93	0.020 32	0.172 02	0.011 77	0.117 82
In	49	0.009 07	0.019 32	0.171 74	0.011 49	0.115 94
Sn	50	0.008 25	0.018 33	0.172 04	0.011 25	0.114 41
Sb	51	0.007 51	0.017 43	0.172 16	0.010 99	0.112 75
Te	52	0.006 82	0.016 56	0.172 60	0.010 76	0.111 22
I	53	0.006 19	0.015 73	0.173 13	0.010 52	0.109 81
Xe	54	0.005 62	0.014 93	0.173 85	0.010 30	0.108 51
W	74	0.000 70	0.004 94	0.208 35	0.006 89	0.094 41
Au	79	0.000 40	0.003 60	0.226 75	0.006 39	0.094 96
Th	90	0.000 11	0.001 73	0.280 48	0.005 51	0.099 84
U	92	0.000 09	0.001 51	0.292 59	0.005 38	0.101 25

$$r \to r(1 - \alpha_d \{1 - \exp[-(r/r_c)^3]\}/r^3) \qquad (11)$$

in the dipole transition moment $(nlj \mid r \mid n'l'j')$, i.e., the integral of Eq. (10). The effective cutoff radius r_c is taken equal to the core radius predicted by the Hartree-Slater approximation, i.e., equal to r_1 above.

As discussed earlier, core polarization affects the calculation of transition matrix elements for valence electrons in two ways: it changes the wave functions and their energies themselves, and, more importantly, it changes the effective transition operator. Due to the nature of our treatment, the polarization potential, with leading term $1/r^4$, has a small effect on the wave function. We found, however, the change in the dipole operator was significant. There has been some controversy in the literature about the arbitrariness of choice for the cutoff radius r_c. Our choice of r_c to be the Hartree-Slater, or Dirac-Slater for heavier atoms, core radius of the atom or ion is unique as well as physically interpretable. The excellent agreement of our results with accurate experiments provides a further justification of this choice. We did repeat the calculations for most of the ions using the Dirac-Slater[46] rather than the Hartree-Slater potential, but the results were essentially identical.

VI. RESULTS

Our calculations for lifetimes and oscillator strengths for $n = 3$ levels are presented in Tables III and IV and compared with critically selected experimental results in Tables I and V. Table I presents the $3p$ lifetimes and favors cascade-free and ANDC measurements for presentation. The agreement between computation and measurement is to within experimental uncertainties. For the $3d$ levels, ANDC measurements have only been made for S VI (Ref. 17) and their agreement with the present calculations is excellent. The other results cited were obtained by simple curve-fitting methods; thus the experimental $3d$ lifetimes tend to be longer than the theoretical predictions, which is almost certainly a result of unaccounted cascade repopulation in the experimental decay curves. An ANDC analysis incorporating the $3d$-$4f$ (and possibly other) decay curves into the $3p$-$3d$ analysis could do much to elucidate this problem.

The single-configuration Dirac-Fock (DF) calculations of Kim and Cheng,[6] also shown in Table I, give systematically shorter lifetimes than our values and are in the opposite direction from the experimental trend. We further discuss this behavior below within the context of oscillator strengths.

Table V compares the present results for $3s$-$3p$ absorption oscillator strengths with those obtained by inverting measured $3p$ lifetimes, as well as the DF calculations of Kim and Cheng[6] and Karwowski and Szulkin,[47] and the MCHF calculations of Froese-Fischer[5] which included core-polarization and correlation effects. Figure 3 presents a plot of the individual line and multiplet absorption oscillator strengths versus $1/Z$.

TABLE V. Experimental and theoretical oscillator strengths for the $3s\,{}^2S - 3p\,{}^2P$ transitions in the Na isoelectronic sequence.

Ion	Upper level	Experiment		Theory	
		ANDC	Other	Present	Other
Na I	$3p\,{}^2P_{1/2}$		0.3179(5)[a]	0.3180	0.329[b]
	$3p\,{}^2P_{3/2}$		0.6310(15)[a,c]	0.6365	0.658[b]
	multiplet		0.9489(21)[a,c]	0.9545	0.987[b]
					0.965[d]
Mg II	$3p\,{}^2P_{1/2}$		0.295(22)[e]	0.3043	0.318[b]
	$3p\,{}^2P_{3/2}$		0.589(44)[e]	0.6103	0.637[b]
	multiplet		0.884(49)[e]	0.9146	0.955[b]
					0.913[d]
S VI	$3p\,{}^2P_{1/2}$	0.23(1)[f]		0.2163	
	$3p\,{}^2P_{3/2}$	0.44(2)[f]		0.4384	
	multiplet	0.66(2)[f]		0.6547	0.651[d]
Cl VII	$3p\,{}^2P_{1/2}$	0.195(8)[g]		0.2010	
	$3p\,{}^2P_{3/2}$	0.409(9)[g]		0.4090	
	multiplet	0.603(15)[g]		0.6100	0.604[d]
Ar VIII	$3p\,{}^2P_{1/2}$	0.183(4)[h]		0.1865	0.196[b]
	$3p\,{}^2P_{3/2}$	0.378(10)[h]		0.3813	0.401[b]
	multiplet	0.561(11)[h]		0.5678	0.598[b]
					0.566[c]
Ti XII	$3p\,{}^2P_{1/2}$	0.143(9)[i]		0.1550	0.152[b]
	$3p\,{}^2P_{3/2}$	0.312(19)[i]		0.3220	0.327[b]
	multiplet	0.455(21)[i]		0.4770	0.479[b]
					0.428[j]
Fe XVI	$3p\,{}^2P_{1/2}$	0.115(9)[i]	0.124[k]	0.120	0.125[b]
					0.125[l]
	$3p\,{}^2P_{3/2}$	0.244(15)[i]		0.261	0.272[b]
		0.244[m]			0.271[l]
	multiplet	0.358(17)[i]		0.381	0.397[b]
		0.368[m]			0.383[d]
					0.332[j]
Ni XVIII	$3p\,{}^2P_{1/2}$	0.109(7)[i]	0.114[m]	0.111	
	$3p\,{}^2P_{3/2}$	0.226(16)[i]	0.237[m]	0.245	
	multiplet	0.335(16)[i]	0.351[m]	0.356	
Cu XIX	$3p\,{}^2P_{1/2}$	0.112(07)[i]	0.112[n]	0.106	
			0.16[o]		
	$3p\,{}^2P_{3/2}$			0.238	
	multiplet			0.344	

[a]A. Gaupp et al., Ref. 12; Refs. 12 and 22 provide a comprehensive bibliography for the Na states.
[b]Y.-K. Kim and K.-T. Cheng, Ref. 6.
[c]W. Gawlik et al., Ref. 13.
[d]C. Froese-Fischer, Ref. 5.
[e]L. Lundin et al., Ref. 22.
[f]J. O. Ekberg et al., Ref. 17.
[g]C. Jupén et al., Ref. 18.
[h]N. Reistad et al., Ref. 19.
[i]R. Hutton et al., Ref. 20.
[j]E. Biémont, Ref. 8.
[k]J. P. Buchet et al., Ref. 21.
[l]J. Karwowski and M. Szulkin, Ref. 47.
[m]D. J. Pegg et al., Ref. 26.
[n]D. J. Pegg et al., Ref. 27.
[o]M. C. Buchet-Poulizac and J. P. Buchet, Ref. 28.

Our values are in agreement with all the experimental values to within their error limits. This is also the case for the multiplet values of the MCHF calculation,[5] which fails in the case of Na for the reasons discussed above in the context of Fig. 1. The excellent agreement between our values and those of Ref. 5, though gratifying, is not surprising to us because both approaches account for the same major effect, i.e., core polarization by the valence electron. The MCHF method includes it through a multiconfiguration treatment, whereas our method introduces it through the effective core polarizability α_d. The discussion at the end of Sec. IV, however, indicates that the MCHF results will worsen beyond Fe, since it then becomes necessary to use different radial wave functions for $3p_{1/2}$ and $3p_{3/2}$.

We believe that the present approach yields accurate oscillator strengths and lifetimes, at least in the cases where Rydberg series are not perturbed. This was already demonstrated for the alkali-metal atoms, [29] He I,[48,49] Li II,[50] Cu II,[51] and Ag II.[51] It is our hope that the results of this work will stimulate further accurate ex-perimental investigations, especially at larger atomic numbers. The theoretical study of the Cu I and Li I isoelectronic sequences is currently in progress.

Finally, in view of the controversy and the uncertainties that are introduced both in theoretical and experimental determinations of lifetimes and oscillator strengths due to the energy factors involved [cf. Eqs. (8) and (9)], we recommend that values of the line strengths $S(\gamma J, \gamma' J')$ [cf. Eq. (10)] be given instead, which are free from those factors.

[1]R. J. S. Crossley, L. J. Curtis, and C. Froese-Fischer, Phys. Lett. 57A, 220 (1976).

[2]S. M. Younger and W. L. Wiese, Phys. Rev. A 18, 2366 (1978).

[3]L. J. Curtis, H. G. Berry, and J. Bromander, Phys. Lett. 34A, 169 (1971).

[4]L. J. Curtis, in Beam-Foil Spectroscopy, edited by S. Bashkin (Springer-Verlag, Berlin, 1976), pp. 63–109.

[5]C. Froese-Fischer, Can. J. Phys. 54, 1465 (1976).

[6]Y.-K. Kim and K.-T. Cheng, J. Opt. Soc. Am. 68, 836 (1978).

[7]R. P. McEachran and M. Cohen, J. Phys. B 16, 3125 (1983).

[8]E. Biémont, Physica 85C, 393 (1977).

[9]J. Karwowski and M. Szulkin, J. Phys. B 14, 1915 (1981).

[10]V. P. Shevelko, Opt. Spectrosk. 36, 7 (1974).

[11]C. Laughlin, M. N. Lewis, and Z. J. Horak, Astrophys. J. 197, 799 (1975).

[12]A. Gaupp, P. Kuske, and H. J. Andrä, Phys. Rev. A 26, 3351 (1982).

[13]W. Gawlik, J. Kowalski, R. Neumann, H. B. Wiegemann, and K. Winkler, J. Phys. B 12, 3873 (1979).

[14]L. Engström, Nucl. Instrum. Methods 202, 369 (1982).

[15]K. Weckström, Phys. Scr. 23, 849 (1981).

[16]E. H. Pinnington and R. N. Gosselin, J. Phys. (Paris) Colloq. 40, CI-149 (1979).

[17]J. O. Ekberg, L. Engström, S. Bashkin, B. Denne, S. Huldt, S. Johansson, C. Jupén, U. Litzén, A. Trigueiros, and I. Martinson, Phys. Scr. 27, 425 (1983).

[18]C. Jupén, L. Engström, S. Huldt, A. Trigueiros, J. O. Ekberg, U. Litzén, and I. Martinson, Phys. Scr. 29, 226 (1984).

[19]N. Reistad, L. Engström, and H. G. Berry, Phys. Scr. 34, 158 (1986).

[20]R. Hutton, L. Engström and E. Träbert, Phys. Rev. Lett. 60, 2469 (1988).

[21]J. P. Buchet, M. C. Buchet-Poulizac, A. Denis, J. Desesquelles, and M. Druetta, Phys. Rev. A 22, 2061 (1980).

[22]L. Lundin, B. Engman, J. Hilke, and I. Martinson, Phys. Scr. 8, 274 (1973).

[23]E. H. Pinnington, R. N. Gosselin, J. A. O'Neill, J. A. Ker-nahan, K. E. Donnelly, and R. L. Brooks, Phys. Scr. 20, 151 (1979).

[24]M. C. Buchet-Poulizac, J. P. Buchet, and P. Ceyzeriat, Nucl. Instrum. Methods 202, 13 (1982).

[25]R. Hutton, L. Engström, and E. Träbert, Nucl. Instrum. Methods Phys. Res., Sect. B 31, 294 (1988).

[26]D. J. Pegg, P. M. Griffin, B. M. Johnson, K. W. Jones, and T. H. Krause, Astrophys. J. 224, 1056 (1978).

[27]D. J. Pegg, P. M. Griffin, B. M. Johnson, K. W. Jones, J. L. Cecchi, and T. H. Krause, Phys. Rev. A 16, 2008 (1977).

[28]M. C. Buchet-Poulizac and J. P. Buchet, Nucl. Instrum. Methods Phys. Res., Sect. B 31, 182 (1988).

[29]C. E. Theodosiou, Phys. Rev. A 30, 2881 (1984).

[30]F. Herman and S. Skillman, Atomic Structure Calculations (Prentice-Hall, Englewood Cliffs, NJ, 1963); J. P. Desclaux, Comput. Phys. Commun. 1, 216 (1969).

[31]P. Risberg, Ark. Fys. 10, 583 (1956); 9, 483 (1955).

[32]B. Isberg, Ark. Fys. 35, 551 (1968).

[33]Y. G. Toresson, Ark. Fys. 17, 179 (1960).

[34]C. E. Magnusson and P. O. Zetterberg, Phys. Scr. 10, 177 (1974).

[35]I. Joelsson, P. O. Zetterberg, and C. E. Magnusson, Phys. Scr. 20, 145 (1979).

[36]C. Jupén and J. Fremberg, Phys. Scr. 30, 260 (1984).

[37]J. Reader, V. Kaufman, J. Sugar, J. O. Ekberg, U. Feldman, C. M. Brown, J. F. Seely, and W. L. Rowan, J. Opt. Soc. Am. B 4, 1821 (1987).

[38]B. Edlén, Phys. Scr. 17, 565 (1978).

[39]C. M. Brown, J. F. Seely, U. Feldman, M. C. Richardson, W. E. Behring, and L. Cohen, J. Opt. Soc. Am. B 3, 701 (1986).

[40]I. P. Grant, B. J. McKenzie, P. H. Norrington, D. F. Mayers, and N. C. Pyper, Comput. Phys. Commun. 21, 207 (1980).

[41]A. Lindgård and S. E. Nielsen, At. Data Nucl. Data Tables 19, 533 (1977).

[42]W. R. Johnson, D. Kolb, and K.-N. Huang, At. Data Nucl. Data Tables 28, 333 (1983).

[43]D. R. Bates and A. Damgaard, Philos. Trans. R. Soc. London

A **242**, 101 (1949).

[44]I. B. Bersuker, Opt. Spektrosk. **3**, 97 (1957).

[45]S. Hameed, A. Herzenberg, and M. G. James, J. Phys. B **1**, 822 (1968).

[46]D. A. Lieberman, D. T. Cromer, and J. T. Waber, Comput. Phys. Commun. **2**, 107 (1971).

[47]J. Karwowski and M. Szulkin, J. Phys. B **14**, 1915 (1981).

[48]C. E. Theodosiou, Phys. Rev. A **30**, 2910 (1984).

[49]C. E. Theodosiou, At. Data Nucl. Data Tables **36**, 97 (1987).

[50]C. E. Theodosiou, Phys. Scr. **32**, 129 (1985).

[51]C. E. Theodosiou, J. Opt. Soc. Am. B **3**, 1107 (1986).